

Dopamine synthesis capacity correlates with mu-opioid receptor availability in the human basal ganglia: a triple-tracer PET study

Joonas Majuri^{a,b,c}, Juho Joutsa^{a,b,d,e}, Eveliina Arponen^c, Sarita Forsback^c, Valtteri Kaasinen^{a,b,c}

- a. Division of Clinical Neurosciences, Turku University Hospital, PO Box 52, FIN-20521 Turku, Finland
- b. Department of Neurology, University of Turku, PO Box 52, FIN-20521 Turku, Finland
- c. Turku PET Centre, University of Turku, PO Box 52, FIN-20521 Turku, Finland
- d. Athinoula A. Martinos Center for Biomedical Imaging, Massachusetts General Hospital and Harvard Medical School, Charlestown, MA
- e. Berenson-Allen Center for Noninvasive Brain Stimulation, Beth Israel Deaconess Medical Center and Harvard Medical School, Boston, MA

Corresponding author

Dr. Joonas Majuri

Turku PET Centre

POB 52, FIN-20521 Turku

Finland

Tel. +358-(0)-23133000

Email: joeema@utu.fi

Declarations of interest: none

Abstract

Animal studies have suggested that dopamine and opioid neurotransmitter systems interact in brain regions that are relevant for reward functions, but data in humans are very limited. The interaction is potentially important in disorders affecting these neurotransmitter systems, such as addiction. Here, we investigated whether subcortical μ -opioid receptor (MOR) availability and presynaptic dopamine synthesis capacity are correlated in the healthy human brain or in pathological gamblers (PGs) using positron emission tomography with 6- ^{18}F fluoro-L-dopa and ^{11}C carfentanil. The specificity of the findings was further investigated by including a serotonin transporter ligand, ^{11}C MADAM, as a negative control. Thirteen PG patients and 15 age-, sex- and weight-matched controls underwent the scans. In both groups, presynaptic dopamine synthesis capacity was associated with MOR availability in the putamen, caudate nucleus and globus pallidus. No similar associations were observed between dopamine synthesis capacity and ^{11}C MADAM binding, supporting a specific interplay between presynaptic dopamine neurotransmission and opioid receptor function in the basal ganglia. Correlations were similar between the groups, suggesting that the dopamine-opioid link is general and unaffected by behavioral addiction. The results provide *in vivo* human evidence of a connection between endogenous opioid and dopamine signaling in the brain.

Keywords: dopamine, opioid, pathological gambling, positron emission tomography

1. Introduction

Dopamine and opioid systems both play key roles in the brain reward system (Noble et al., 2015; Volkow et al., 2011). Dopamine is known to be involved in reward anticipation and prediction error signaling, and it is released in the nucleus accumbens after administration of several drugs of abuse (Schultz, 2002; Volkow et al., 2011). The brain opioid system is involved in hedonic processes, and it regulates both reward and loss responses (Laurent et al., 2015; Petrovic et al., 2008). Altered brain dopamine and opioid function have been suggested to play a critical role in pathological gambling (PG), a form of behavioral addiction (Boileau et al., 2014; Clark, 2014; Joutsa et al., 2012; Mick et al., 2016; van Holst et al., 2018). In addition, opioid antagonist medications have shown some efficacy in the treatment of PG (Bullock and Potenza, 2012). Although dopamine and opioid systems are both important for reward functions, it is unclear whether they act independently or if the two systems are modulated by each other. From a therapeutic point of view, the possible connection between dopamine and opioid systems in addictions is important since indirect pharmacological modulation of dopamine neurotransmission using drugs targeting the opioid system may provide a potentially effective treatment for addictions without the marked side effects associated with dopamine antagonists (Noble et al., 2015; Potenza et al., 2011).

In animals, opioidergic drugs have been shown to increase dopaminergic output in the ventral tegmental area (VTA) by μ -opioid receptor (MOR)-mediated hyperpolarization of the inhibitory gamma-aminobutyric acid (GABA) cells (Jalabert et al., 2011; Johnson and North, 1992; Madhavan et al., 2010; Spanagel et al., 1992). Similarly, human neuroimaging studies have shown that pharmacological modification of brain opioid function leads to changes in striatal postsynaptic dopamine D2 receptor affinity, which has been speculated to reflect changes in synaptic dopamine levels (Hagelberg et al., 2002; Spreckelmeyer et al., 2011).

However, there are also negative results (Wang et al., 1997a), and pharmacological treatment of addictions using medication targeting the opioid system has been shown to result in no changes in dopamine receptor binding as measured with [^{11}C]raclopride positron emission tomography (PET) (Daglish et al., 2008; Wang et al., 1997a; Watson et al., 2014). Furthermore, [^{11}C]raclopride binding can reflect either synaptic dopamine levels or D2 receptor availability/affinity, leaving the nature of the opioid-dopamine interaction unclear. Animal studies have suggested that dopaminergic stimulation leads to opioid release (Olive et al., 2001; Soderman and Unterwald, 2009) but the data in humans has remained somewhat inconclusive (Colasanti et al., 2012; Guterstam et al., 2013). A recent PET study showed a correlation between MOR availability and postsynaptic dopamine D2 receptor availability in the ventral striatum (VST) and dorsal caudate nucleus in healthy controls, suggesting that the MOR system is linked to postsynaptic dopamine D2 receptors (Tuominen et al., 2015). In summary, previous studies investigating the opioid-dopamine interaction have focused on postsynaptic dopamine receptor binding as an indicator of dopaminergic function, and the results are somewhat mixed, not allowing for definitive conclusions about the mechanisms of the dopamine-opioid interaction.

Given the lack of data on the interaction between striatal presynaptic dopamine and opioid neurotransmission and their critical role in addiction, we aimed to investigate relationships between presynaptic dopamine function and opioid neurotransmission with PET. We hypothesized that striatal dopamine synthesis capacity, as measured with 6- ^{18}F fluoro-L-dopa (^{18}F fluorodopa) PET, would correlate with MOR binding, as measured with [^{11}C]carfentanil PET. As serotonin transporter (SERT) should not be expressed in dopaminergic neurons, [^{11}C]MADAM binding was included as a negative control (Amara and Kuhar, 1993; Glatt and Reus, 2003; Rothman and Baumann, 2003). To investigate these

associations in the context of addiction, we studied the same connections in a separate sample of individuals with pathological gambling, a form of behavioral addiction without confounding effects of long-term substance use.

2. Methods

This study was conducted in accordance with the Declaration of Helsinki. The study was approved by the local Ethics Committee. All subjects signed written informed consent prior to participation.

2.1. *Subjects*

The demographic data of the studied subjects are presented in Table 1. The subjects in this study were derived from our previous studies that investigated dopamine, opioid and serotonin function in behavioral addictions (Majuri et al., 2017a; Majuri et al., 2017b). The groups did not differ in terms of age, sex, body mass index or alcohol consumption, but differences were observed in smoking ($p=0.067$) and depression scores ($p<0.001$) (Table 1). Fifteen healthy controls (HCs) and 13 PG patients successfully completed both [^{18}F]fluorodopa and [^{11}C]carfentanil PET imaging and were included in this study. One included PG patient lacked [^{11}C]MADAM data. The main exclusion criteria included any clinically significant somatic or psychiatric disorder (apart from PG), any drug addiction or abuse, current pregnancy and prior PET imaging. None of the included subjects used medications known to affect to dopaminergic, opioidergic or serotonergic neurotransmission.

2.2. *Radiochemistry and imaging*

The production procedures for the tracers used have been described in detail previously (Forsback et al., 2009; Halldin et al., 2005; Hirvonen et al., 2009). The radioligand production followed the EU Good Manufacturing Practice regulations at the Turku PET Centre. The radiochemical purity exceeded 95% in all production runs.

The PET scans were performed using a high-resolution research tomograph PET scanner (HRRT, Siemens Medical Solutions, Knoxville), TN, USA) in 3D mode with scatter correction. A transmission scan was performed before each dynamic scan using ^{137}Cs rotating point source. All three PET scans were performed during the same day at fixed intervals. An individually shaped thermoplastic mask was used to minimize head movements during scanning, and head movements were also followed using a stereotaxic infrared camera (Polaris Vicra, Northern Digital, Waterloo, Canada). Two PG patients used a Velcro strap instead because they did not tolerate the thermoplastic mask. For structural reference, 3D T1-weighted MRI scans were obtained using a 3T PET-MRI scanner Philips Ingenuity (Philips Healthcare, Cleveland, OH, USA) with a 34-channel receiving head coil and a sagittal TFE sense pulse sequence (TR 8.1 ms, TE 3.7 ms, flip angle 7° , matrix 256×256 , 176 slices, $1 \times 1 \times 1$ mm voxels).

2.3. Preprocessing

Preprocessing of the images was performed using SPM8 software running on MATLAB R2012a (MathWorks, Natick, MA, USA). Individual PET frames were realigned using a mutual information algorithm to estimate and compensate for head movement during the PET data acquisition. Based on Polaris Vicra infrared camera data, two [^{18}F]fluorodopa scans, three [^{11}C]carfentanil scans and four [^{11}C]MADAM scans showed excessive intra-frame head movements, and individual multiple-acquisition frame reconstructions were made for these nine scans. The core of individual reconstructions was that the PET list mode data were divided to new subframes using a maximum amplitude of 2.5 mm as a threshold (Johansson et al., 2016). Realigned PET images were coregistered with individual T1-weighted MR images. Regions-of-interest (ROIs) were determined using automated

parcellation by FreeSurfer software (version 5.3.0, <http://surfer.nmr.mgh.harvard.edu/>) (Desikan et al., 2006; Fischl et al., 2002) and used to calculate average time-activity curves of all voxels within each ROI. A Patlak plot was used to calculate [^{18}F]fluorodopa influx constant rates (K_i), and a simplified reference tissue model (SRTM) was used to calculate the ratios specifically relative to the non-displaceable binding (BP_{ND}) with [^{11}C]carfentanil and [^{11}C]MADAM (Gunn et al., 1997; Patlak and Blasberg, 1985). The occipital cortex was designated as the reference region for [^{18}F]fluorodopa and [^{11}C]carfentanil, and the cerebellar cortex was designated for [^{11}C]MADAM. The calculated parametric BP_{ND} and K_i images were first warped to the Montreal Neurological Institute standard space (MNI152) using the DARTEL normalization algorithm (Ashburner, 2007) and then smoothed with a Gaussian kernel of 8 mm at full-width and half-maximum to improve the signal-to-noise ratio.

2.4. Statistics

Statistical analyses were performed using both ROI-based methods and voxel-by-voxel approach. ROI analyses were run using SPSS (IBM SPSS Statistics, version 22, Armonk, NY, USA). Because of a suboptimal signal-to-noise ratio and reliability of [^{18}F]fluorodopa in cortical regions (Martin et al., 1989), the analyses were restricted to the amygdala, caudate nucleus, globus pallidus, hippocampus, nucleus accumbens, putamen, and thalamus. The primary analysis followed the general linear model (GLM) using [^{18}F]fluorodopa K_i as a dependent variable and [^{11}C]carfentanil and group as independent variables. The assumptions for GLM were verified by using Levene's test and visual inspection of the variables and model residual distributions. It should be noted that Levene's test was significant in the putamen ($p=0.03$) and caudate ($p=0.04$). The robustness of the associations between regional [^{18}F]fluorodopa and [^{11}C]carfentanil uptake were verified in each group separately by using Spearman's rank order correlation coefficients. In the ROI

analyses, Bonferroni correction was applied to account for multiple comparisons due to 7 analyzed ROIs. The analyses were replicated using Beck Depression Inventory (BDI) score and smoking status as covariates. P-values less than 0.05 were considered significant. Similarly, the association of [¹⁸F]fluorodopa with [¹¹C]MADAM was analyzed using GLM and in the groups separately using Spearman's rank order correlation coefficients.

To confirm the ROI-based results, analogous voxel-by-voxel analyses were conducted using VoxelStats MATLAB package (Mathotaarachchi et al., 2016) running on MATLAB R2016a (MathWorks, Natick, MA, USA). This program enables voxel-wise general linear model calculations with multiple volumetric imaging modalities and correction for multiple comparisons based on random field theory (RFT). Voxel-by-voxel –analysis was conducted with a mask, which was created using the Human Atlas AAL library in WFU Pick Atlas toolbox (Maldjian et al., 2003). The mask included the basal ganglia, thalamus, amygdala and hippocampus, and all brain regions with [¹⁸F]fluorodopa $K_i \geq 0.005$. In the voxel-by-voxel analyses, the association of [¹⁸F]fluorodopa K_i to [¹¹C]carfentanil BP_{ND} values and group effects within each voxel included in the mask were investigated using GLM. Family-wise error-corrected p values less than 0.05 with a cluster-forming threshold of $p < 0.001$ were considered significant, as suggested in the original publication of the software package (Mathotaarachchi et al., 2016).

3. Results

There was no significant interaction between group and [^{11}C]carfentanil BP_{ND} or a group effect on [^{18}F]fluorodopa K_i . However, [^{18}F]fluorodopa K_i was associated with [^{11}C]carfentanil BP_{ND} in the caudate nucleus ($p=0.002$, Bonferroni-corrected $p=0.013$), putamen ($p=0.001$, Bonferroni-corrected $p=0.005$) and globus pallidus ($p<0.001$, Bonferroni-corrected $p=0.002$). When the groups were investigated separately, [^{18}F]fluorodopa K_i and [^{11}C]carfentanil BP_{ND} correlated in the globus pallidus, putamen and caudate nucleus in the HC group (Table 2, Figure 1). In PG patients, similar correlations were observed in the globus pallidus and putamen (Table 2, Figure 1). After Bonferroni correction across the whole sample, Spearman correlation coefficients remained significant in the globus pallidus and putamen (Table 2). Significant correlations between [^{18}F]fluorodopa K_i and [^{11}C]carfentanil BP_{ND} remained in the caudate nucleus ($p=0.007$, Bonferroni-corrected $p=0.022$), putamen ($p=0.004$, Bonferroni-corrected $p=0.011$) and globus pallidus ($p<0.001$, Bonferroni-corrected $p=0.001$) when smoking status was added as a covariate. In addition, BDI score as a covariate did not change the results (caudate nucleus $p=0.003$, Bonferroni-corrected $p=0.010$, putamen $p=0.003$, Bonferroni-corrected $p=0.008$ and globus pallidus $p<0.001$, Bonferroni-corrected $p=0.001$). As expected, no correlations between [^{18}F]fluorodopa K_i and [^{11}C]MADAM BP_{ND} were found in any of the studied ROIs. In parallel to the ROI results, voxel-wise analyses showed no significant group \times [^{11}C]carfentanil BP_{ND} interaction or group effect, but [^{18}F]fluorodopa K_i was associated with [^{11}C]carfentanil BP_{ND} bilaterally in the caudate nucleus (cluster size 8.16 cm^3 , peak voxel at 9, 13.5, 15 mm, $T_{\text{max}}=7.79$) and in the left putamen (cluster size 0.45 cm^3 , peak voxel at -31.5, -3, 7.5 mm, $T_{\text{max}}=4.61$) (Figure 2).

4. Discussion

This study shows that presynaptic dopamine synthesis capacity is correlated with MOR binding in the basal ganglia in the living human brain. Associations between dopamine and opioid systems were detected in both healthy individuals and patients with pathological gambling, indicating a general neurobiological phenomenon that is unaffected by behavioral addiction. Furthermore, the lack of correlations between presynaptic dopamine synthesis capacity and the serotonin transporter ligand [¹¹C]MADAM underscores the specificity of the dopamine-opioid interaction.

Notably, the association between dopamine and opioid function was not uniform across all basal ganglia structures. Our results corroborate the findings by Tuominen et al. (2015) that demonstrated a regionally selective correlation in the ventral striatum and caudate nucleus with MOR and postsynaptic dopamine D2 receptor binding. This regional selectivity may be caused by specific functions of the direct and indirect pathways in regulating dopaminergic neurotransmission. A group of medium spiny neurons in the striatum express dopamine D1 receptors, and these neurons have been considered as direct pathway neurons, projecting to the globus pallidus interna and the pars reticulata of the substantia nigra, whereas D2 receptor-expressing cells are considered to be part of the indirect striatal pathway, sending fibers to the globus pallidus externa and the subthalamic nucleus (Gerfen et al., 1990; Yager et al., 2015). Previously, dopamine D2 receptors and postsynaptic MORs have been shown to exist at the same dopaminergic cells, and MOR-expressing dendritic spines receive convergent inputs from dopaminergic terminals forming asymmetric excitatory synapses (Ambrose et al., 2004; Wang et al., 1997b). Additionally, MOR-rich striatal areas have previously been shown to receive dopaminergic afferents from the substantia nigra (Gerfen et al., 1987), and the MOR distribution and amount of binding sites in the striatum are linked

to striatal dopamine afferents (Caboche et al., 1991). Thus, as the correlation of postsynaptic MOR availability with presynaptic dopamine function was limited to the same striatal regions, the opioid-dopamine interaction observed in this study may reflect the indirect pathway. This is supported by a recent study showing positive correlation of dopamine synthesis capacity with D2 receptor binding but not with dopamine release in the striatum (Berry et al., 2018). However, the pre- and postsynaptic distribution of MORs appears more complex. [¹¹C]Carfentanil uptake is partly affected by presynaptic binding in nerve terminals, and thus, the binding does not only reflect postsynaptic tracer binding (Arvidsson et al., 1995; Gracy et al., 1997; Henderson, 2015). Presynaptic MORs may mediate synaptic transmission either by inhibiting or activating neural activity. For example, in the nucleus accumbens, presynaptic MOR activation seems to lead to a reduction in NMDA, an excitatory glutamate receptor, signaling (Martin et al., 1997). Additional variability comes from the fact that [¹¹C]carfentanil BP_{ND} can be affected by both MOR availability/affinity and synaptic opioid release.

In investigations of brain reward functions, pathological gambling serves as an interesting and unique model, allowing for the examination of brain neurotransmission in addiction without the confounding pharmacological effects of drugs. Previously, as in substance use disorders, altered mesolimbic dopamine release has been suggested to play a critical role in PG (Clark, 2014), but pharmacological interventions targeting the dopamine system have mostly failed (Bullock and Potenza, 2012). However, opioid antagonists have shown some efficacy in the treatment of pathological gambling (Bullock and Potenza, 2012). Our results demonstrate that the dopamine-opioid interaction in the striatum remains intact in PG, which may be a prerequisite for the modulation of the mesolimbic dopamine system by opioidergic

pharmacotherapies. Expanding this work to the dopamine-opioid association in substance addictions would be an interesting area of research in the future.

In addition to dopamine and opioid neurotransmitter systems, there is also evidence of the role of serotonin in reward processing (Daw et al., 2002; Kranz et al., 2010). Preclinical studies have reported direct serotonergic synapsing from dorsal raphe nuclei to VTA dopaminergic cells (Hervé et al., 1987; Van Bockstaele et al., 1994). However, recent animal studies have shown that the majority of the connections between raphe nuclei and VTA, which participate to reward processing, are not serotonergic as assumed, but these connections seem to be mostly glutaminergic, and serotonin acts if co-released with glutamate (Liu et al., 2014; McDevitt et al., 2014; Qi et al., 2014). Further, monoaminergic cells express only their corresponding transporter (Amara and Kuhar, 1993; Glatt and Reus, 2003; Rothman and Baumann, 2003) which can, however, transfer other monoamines into the cell if the corresponding transporters are damaged (Yamada et al., 2007; Zhou et al., 2002). Thus, although there is interplay between the serotonin and dopamine systems, we assumed that the regional dopamine synthesis rate would not correlate with SERT density, which was confirmed by our analyses. The association of [¹⁸F]fluorodopa K_i and [¹¹C]carfentanil BP_{ND} therefore likely reflects a true association between these neurotransmitter systems and is not caused by general factors that could increase or decrease uptake/binding of all the tracers.

In our previous studies, we have reported group differences using [¹⁸F]fluorodopa, [¹¹C]carfentanil and [¹¹C]MADAM in the same HC and PG subjects analyzed in the present study. There were no differences in presynaptic dopamine synthesis rates or MOR and SERT availabilities between the PG and HC groups. However, patients with binge eating

disorder (BED), another behavioral addiction, showed significant decreases in [^{18}F]fluorodopa and [^{11}C]carfentanil binding along with regionally altered [^{11}C]MADAM binding (Majuri et al., 2017a; Majuri et al., 2017b). In the present study, we focused on associations between dopamine synthesis capacity and MOR availability while using SERT binding as a control but decided to not include BED patients because of the small number of BED patients available for correlation analyses ($n=7$). It should be noted that, apart from the dopamine-producing neurons, [^{18}F]fluorodopa may be converted to dopamine in other monoaminergic neurons as well, and thus part of the signal may stem from other monoamine systems in brain regions with low density of dopamine neurons (Brown et al., 1999). However, in the dopamine-rich striatum, the signal can be considered to be mostly dopaminergic (Lloyd and Hornykiewicz, 1970; Martin et al., 1989).

The present study has its strengths and weaknesses. As strengths, we used a PET scanner with high spatial resolution, our findings were derived from 83 brain PET scans and were consistent in two independent groups, and voxel-based analyses confirmed the ROI findings in the striatum. Furthermore, the correlations were not driven by confounding factors, such as smoking or depression, and no association between [^{18}F]fluorodopa K_i and [^{11}C]MADAM BP_{ND} were found, which underscores the specificity of the findings. However, it should be noted that only baseline neurotransmitter activity at rest was measured, not possible stimulus-dependent dynamic changes in the synaptic neurotransmitter levels or receptor availability. Second, voxel-based methods could not confirm the correlation between [^{18}F]fluorodopa and [^{11}C]carfentanil in one region, the globus pallidus. This could be due to the spatial smoothing and increased signal-to-noise ratio, as the size of the globus pallidus is relatively small when compared to the striatum. Additionally, after a conservative Bonferroni correction, ROI-based caudate nucleus correlation coefficients were not

significant although significant in the voxel-wise analysis. Third, even though our sample size with 83 PET scans can be considered to be relatively large in the PET imaging field, it should be noted that a sample size of this magnitude can overestimate true values of correlation coefficients, which need greater samples to stabilize (Schönbrodt and Perugini, 2013). Although the present results should therefore be replicated in larger samples of individuals, the results are supported by preclinical studies showing the co-existence of dopamine and opioid receptors in the striatum. Animal studies have shown the innervation of dopaminergic afferents to the MOR-rich striatal patch regions and that the dopamine afferents are linked to the MOR expression and distribution (Caboche et al., 1991; Gerfen et al., 1987). Furthermore, dopamine D2 receptors and MORs have been found in the same striatal cells (Ambrose et al., 2004; Wang et al., 1997b). Thus, even though the sample size is not ideal for the correlational method, the dopamine-opioid correlation seems robust in relation to the preclinical data.

In conclusion, we have shown novel intraregional correlations between μ -opioid receptor availability and presynaptic dopamine synthesis rate in the human striatum and globus pallidus. Our results highlight that the opioid and dopamine neurotransmitter systems are tightly connected in certain subcortical brain regions. The correlations were unaffected by behavioral addiction, but further multi-tracer studies, particularly in patients with substance addictions, are warranted.

5. Acknowledgements

We thank the staff of the Turku PET Centre for their expertise and assistance in PET and MR imaging. This study was supported by the Academy of Finland (grant # 256836), the Finnish Foundation for Alcohol Studies and Turku University Hospital ERVA grants.

The authors report no conflicts of interest.

6. References

- Amara, S.G., Kuhar, M.J., 1993. Neurotransmitter transporters: recent progress. *Annu Rev Neurosci* 16, 73-93.
- Ambrose, L.M., Unterwald, E.M., Van Bockstaele, E.J., 2004. Ultrastructural evidence for co-localization of dopamine D2 and micro-opioid receptors in the rat dorsolateral striatum. *Anat Rec A Discov Mol Cell Evol Biol* 279, 583-591.
- Arvidsson, U., Riedl, M., Chakrabarti, S., Lee, J.H., Nakano, A.H., Dado, R.J., Loh, H.H., Law, P.Y., Wessendorf, M.W., Elde, R., 1995. Distribution and targeting of a mu-opioid receptor (MOR1) in brain and spinal cord. *J Neurosci* 15, 3328-3341.
- Ashburner, J., 2007. A fast diffeomorphic image registration algorithm. *Neuroimage* 38, 95-113.
- Berry, A.S., Shah, V.D., Furman, D.J., White, R.L., Baker, S.L., O'Neil, J.P., Janabi, M., D'Esposito, M., Jagust, W.J., 2018. Dopamine Synthesis Capacity is Associated with D2/3 Receptor Binding but Not Dopamine Release. *Neuropsychopharmacology* 43, 1201-1211.
- Boileau, I., Payer, D., Chugani, B., Lobo, D.S., Houle, S., Wilson, A.A., Warsh, J., Kish, S.J., Zack, M., 2014. In vivo evidence for greater amphetamine-induced dopamine release in pathological gambling: a positron emission tomography study with [(11)C]-(+)-PHNO. *Mol Psychiatry* 19, 1305-1313.
- Brown, W.D., Taylor, M.D., Roberts, A.D., Oakes, T.R., Schueller, M.J., Holden, J.E., Malischke, L.M., DeJesus, O.T., Nickles, R.J., 1999. FluoroDOPA PET shows the nondopaminergic as well as dopaminergic destinations of levodopa. *Neurology* 53, 1212-1218.
- Bullock, S.A., Potenza, M.N., 2012. Pathological Gambling: Neuropsychopharmacology and Treatment. *Curr Psychopharmacol* 1.
- Caboche, J., Rogard, M., Besson, M.J., 1991. Comparative development of D1-dopamine and mu opiate receptors in normal and in 6-hydroxydopamine-lesioned neonatal rat striatum: dopaminergic fibers regulate mu but not D1 receptor distribution. *Brain Res Dev Brain Res* 58, 111-122.
- Clark, L., 2014. Disordered gambling: the evolving concept of behavioral addiction. *Ann N Y Acad Sci* 1327, 46-61.
- Colasanti, A., Searle, G.E., Long, C.J., Hill, S.P., Reiley, R.R., Quelch, D., Erritzoe, D., Tziortzi, A.C., Reed, L.J., Lingford-Hughes, A.R., Waldman, A.D., Schruers, K.R., Matthews, P.M., Gunn, R.N., Nutt, D.J., Rabiner, E.A., 2012. Endogenous opioid release in the human brain reward system induced by acute amphetamine administration. *Biol Psychiatry* 72, 371-377.
- Daglish, M.R., Williams, T.M., Wilson, S.J., Taylor, L.G., Eap, C.B., Augsburger, M., Giroud, C., Brooks, D.J., Myles, J.S., Grasby, P., Lingford-Hughes, A.R., Nutt, D.J., 2008. Brain dopamine response in human opioid addiction. *Br J Psychiatry* 193, 65-72.
- Daw, N.D., Kakade, S., Dayan, P., 2002. Opponent interactions between serotonin and dopamine. *Neural Netw* 15, 603-616.
- Desikan, R.S., Ségonne, F., Fischl, B., Quinn, B.T., Dickerson, B.C., Blacker, D., Buckner, R.L., Dale, A.M., Maguire, R.P., Hyman, B.T., Albert, M.S., Killiany, R.J., 2006. An automated labeling system for subdividing the human cerebral cortex on MRI scans into gyral based regions of interest. *Neuroimage* 31, 968-980.
- Fischl, B., Salat, D.H., Busa, E., Albert, M., Dieterich, M., Haselgrove, C., van der Kouwe, A., Killiany, R., Kennedy, D., Klaveness, S., Montillo, A., Makris, N., Rosen, B., Dale, A.M., 2002. Whole brain segmentation: automated labeling of neuroanatomical structures in the human brain. *Neuron* 33, 341-355.

- Forsback, S., Eskola, O., Bergman, J., Haaparanta, M., Solin, O., 2009. Alternative solvents for electrophilic synthesis of 6-[18F]fluoro-L-DOPA. *J. Labelled Compd Rad* 52, 286-288.
- Gerfen, C.R., Engber, T.M., Mahan, L.C., Susel, Z., Chase, T.N., Monsma, F.J., Sibley, D.R., 1990. D1 and D2 dopamine receptor-regulated gene expression of striatonigral and striatopallidal neurons. *Science* 250, 1429-1432.
- Gerfen, C.R., Herkenham, M., Thibault, J., 1987. The neostriatal mosaic: II. Patch- and matrix-directed mesostriatal dopaminergic and non-dopaminergic systems. *J Neurosci* 7, 3915-3934.
- Glatt, C.E., Reus, V.I., 2003. Pharmacogenetics of monoamine transporters. *Pharmacogenomics* 4, 583-596.
- Gracy, K.N., Svingos, A.L., Pickel, V.M., 1997. Dual ultrastructural localization of mu-opioid receptors and NMDA-type glutamate receptors in the shell of the rat nucleus accumbens. *J Neurosci* 17, 4839-4848.
- Gunn, R.N., Lammertsma, A.A., Hume, S.P., Cunningham, V.J., 1997. Parametric imaging of ligand-receptor binding in PET using a simplified reference region model. *Neuroimage* 6, 279-287.
- Guterstam, J., Jayaram-Lindström, N., Cervenka, S., Frost, J.J., Farde, L., Halldin, C., Franck, J., 2013. Effects of amphetamine on the human brain opioid system--a positron emission tomography study. *Int J Neuropsychopharmacol* 16, 763-769.
- Hagelberg, N., Kajander, J.K., Någren, K., Hinkka, S., Hietala, J., Scheinin, H., 2002. Mu-receptor agonism with alfentanil increases striatal dopamine D2 receptor binding in man. *Synapse* 45, 25-30.
- Halldin, C., Lundberg, J., Sóvágó, J., Gulyás, B., Guilloteau, D., Vercouillie, J., Emond, P., Chalon, S., Tarkiainen, J., Hiltunen, J., Farde, L., 2005. [(11C)MADAM, a new serotonin transporter radioligand characterized in the monkey brain by PET. *Synapse* 58, 173-183.
- Henderson, G., 2015. The μ -opioid receptor: an electrophysiologist's perspective from the sharp end. *Br J Pharmacol* 172, 260-267.
- Hervé, D., Pickel, V.M., Joh, T.H., Beaudet, A., 1987. Serotonin axon terminals in the ventral tegmental area of the rat: fine structure and synaptic input to dopaminergic neurons. *Brain Res* 435, 71-83.
- Hirvonen, J., Aalto, S., Hagelberg, N., Maksimow, A., Ingman, K., Oikonen, V., Virkkala, J., Någren, K., Scheinin, H., 2009. Measurement of central mu-opioid receptor binding in vivo with PET and [11C]carfentanil: a test-retest study in healthy subjects. *Eur J Nucl Med Mol Imaging* 36, 275-286.
- Jalabert, M., Bourdy, R., Courtin, J., Veinante, P., Manzoni, O.J., Barrot, M., Georges, F., 2011. Neuronal circuits underlying acute morphine action on dopamine neurons. *Proc Natl Acad Sci U S A* 108, 16446-16450.
- Johansson, J., Keller, S., Tuisku, J., Teräs, M., 2016. Performance of an Image-based Motion Compensation Algorithm for the HRRT: a striatum-phantom study with true motion. *IEEE Nucl. Sci. Symp. Med Imaging Conf.*, p. 3.
- Johnson, S.W., North, R.A., 1992. Opioids excite dopamine neurons by hyperpolarization of local interneurons. *J Neurosci* 12, 483-488.
- Joutsa, J., Johansson, J., Niemelä, S., Ollikainen, A., Hirvonen, M.M., Piepponen, P., Arponen, E., Alho, H., Voon, V., Rinne, J.O., Hietala, J., Kaasinen, V., 2012. Mesolimbic dopamine release is linked to symptom severity in pathological gambling. *Neuroimage* 60, 1992-1999.
- Kranz, G.S., Kasper, S., Lanzenberger, R., 2010. Reward and the serotonergic system. *Neuroscience* 166, 1023-1035.
- Laurent, V., Morse, A.K., Balleine, B.W., 2015. The role of opioid processes in reward and decision-making. *Br J Pharmacol* 172, 449-459.

- Liu, Z., Zhou, J., Li, Y., Hu, F., Lu, Y., Ma, M., Feng, Q., Zhang, J.E., Wang, D., Zeng, J., Bao, J., Kim, J.Y., Chen, Z.F., El Mestikawy, S., Luo, M., 2014. Dorsal raphe neurons signal reward through 5-HT and glutamate. *Neuron* 81, 1360-1374.
- Lloyd, K., Hornykiewicz, O., 1970. Parkinson's disease: activity of L-dopa decarboxylase in discrete brain regions. *Science* 170, 1212-1213.
- Madhavan, A., Bonci, A., Whistler, J.L., 2010. Opioid-Induced GABA potentiation after chronic morphine attenuates the rewarding effects of opioids in the ventral tegmental area. *J Neurosci* 30, 14029-14035.
- Majuri, J., Joutsa, J., Johansson, J., Voon, V., Alakurtti, K., Parkkola, R., Lahti, T., Alho, H., Hirvonen, J., Arponen, E., Forsback, S., Kaasinen, V., 2017a. Dopamine and Opioid Neurotransmission in Behavioral Addictions: A Comparative PET Study in Pathological Gambling and Binge Eating. *Neuropsychopharmacology* 42, 1169-1177.
- Majuri, J., Joutsa, J., Johansson, J., Voon, V., Parkkola, R., Alho, H., Arponen, E., Kaasinen, V., 2017b. Serotonin transporter density in binge eating disorder and pathological gambling: A PET study with [*Eur Neuropsychopharmacol* 27, 1281-1288.
- Maldjian, J.A., Laurienti, P.J., Kraft, R.A., Burdette, J.H., 2003. An automated method for neuroanatomic and cytoarchitectonic atlas-based interrogation of fMRI data sets. *Neuroimage* 19, 1233-1239.
- Martin, G., Nie, Z., Siggins, G.R., 1997. μ -Opioid receptors modulate NMDA receptor-mediated responses in nucleus accumbens neurons. *J Neurosci* 17, 11-22.
- Martin, W.R., Palmer, M.R., Patlak, C.S., Calne, D.B., 1989. Nigrostriatal function in humans studied with positron emission tomography. *Ann Neurol* 26, 535-542.
- Mathotaarachchi, S., Wang, S., Shin, M., Pascoal, T.A., Benedet, A.L., Kang, M.S., Beaudry, T., Fonov, V.S., Gauthier, S., Labbe, A., Rosa-Neto, P., 2016. VoxelStats: A MATLAB Package for Multi-Modal Voxel-Wise Brain Image Analysis. *Front Neuroinform* 10, 20.
- McDevitt, R.A., Tiran-Cappello, A., Shen, H., Balderas, I., Britt, J.P., Marino, R.A.M., Chung, S.L., Richie, C.T., Harvey, B.K., Bonci, A., 2014. Serotonergic versus nonserotonergic dorsal raphe projection neurons: differential participation in reward circuitry. *Cell Rep* 8, 1857-1869.
- Mick, I., Myers, J., Ramos, A.C., Stokes, P.R., Erritzoe, D., Colasanti, A., Gunn, R.N., Rabiner, E.A., Searle, G.E., Waldman, A.D., Parkin, M.C., Brailsford, A.D., Galduróz, J.C., Bowden-Jones, H., Clark, L., Nutt, D.J., Lingford-Hughes, A.R., 2016. Blunted Endogenous Opioid Release Following an Oral Amphetamine Challenge in Pathological Gamblers. *Neuropsychopharmacology* 41, 1742-1750.
- Noble, F., Lenoir, M., Marie, N., 2015. The opioid receptors as targets for drug abuse medication. *Br J Pharmacol* 172, 3964-3979.
- Olive, M.F., Koenig, H.N., Nannini, M.A., Hodge, C.W., 2001. Stimulation of endorphin neurotransmission in the nucleus accumbens by ethanol, cocaine, and amphetamine. *J Neurosci* 21, RC184.
- Patlak, C.S., Blasberg, R.G., 1985. Graphical evaluation of blood-to-brain transfer constants from multiple-time uptake data. Generalizations. *J Cereb Blood Flow Metab* 5, 584-590.
- Petrovic, P., Pleger, B., Seymour, B., Klöppel, S., De Martino, B., Critchley, H., Dolan, R.J., 2008. Blocking central opiate function modulates hedonic impact and anterior cingulate response to rewards and losses. *J Neurosci* 28, 10509-10516.
- Potenza, M.N., Sofuoglu, M., Carroll, K.M., Rounsaville, B.J., 2011. Neuroscience of behavioral and pharmacological treatments for addictions. *Neuron* 69, 695-712.
- Qi, J., Zhang, S., Wang, H.L., Wang, H., de Jesus Aceves Buendia, J., Hoffman, A.F., Lupica, C.R., Seal, R.P., Morales, M., 2014. A glutamatergic reward input from the dorsal raphe to ventral tegmental area dopamine neurons. *Nat Commun* 5, 5390.

- Rothman, R.B., Baumann, M.H., 2003. Monoamine transporters and psychostimulant drugs. *Eur J Pharmacol* 479, 23-40.
- Schönbrodt, F., Perugini, M., 2013. At what sample size do correlations stabilize? *Journal of Research in Personality* 47, 609-612.
- Schultz, W., 2002. Getting formal with dopamine and reward. *Neuron* 36, 241-263.
- Soderman, A.R., Unterwald, E.M., 2009. Cocaine-induced mu opioid receptor occupancy within the striatum is mediated by dopamine D2 receptors. *Brain Res* 1296, 63-71.
- Spanagel, R., Herz, A., Shippenberg, T.S., 1992. Opposing tonically active endogenous opioid systems modulate the mesolimbic dopaminergic pathway. *Proc Natl Acad Sci U S A* 89, 2046-2050.
- Spreckelmeyer, K.N., Paulzen, M., Raptis, M., Baltus, T., Schaffrath, S., Van Waesberghe, J., Zalewski, M.M., Rösch, F., Vernaleken, I., Schäfer, W.M., Gründer, G., 2011. Opiate-induced dopamine release is modulated by severity of alcohol dependence: an [(18)F]fallypride positron emission tomography study. *Biol Psychiatry* 70, 770-776.
- Tuominen, L., Tuulari, J., Karlsson, H., Hirvonen, J., Helin, S., Salminen, P., Parkkola, R., Hietala, J., Nuutila, P., Nummenmaa, L., 2015. Aberrant mesolimbic dopamine-opiate interaction in obesity. *Neuroimage* 122, 80-86.
- Van Bockstaele, E.J., Cestari, D.M., Pickel, V.M., 1994. Synaptic structure and connectivity of serotonin terminals in the ventral tegmental area: potential sites for modulation of mesolimbic dopamine neurons. *Brain Res* 647, 307-322.
- van Holst, R.J., Sescousse, G., Janssen, L.K., Janssen, M., Berry, A.S., Jagust, W.J., Cools, R., 2018. Increased Striatal Dopamine Synthesis Capacity in Gambling Addiction. *Biol Psychiatry* 83, 1036-1043.
- Volkow, N.D., Wang, G.J., Fowler, J.S., Tomasi, D., Telang, F., 2011. Addiction: beyond dopamine reward circuitry. *Proc Natl Acad Sci U S A* 108, 15037-15042.
- Wang, G.J., Volkow, N.D., Fowler, J.S., Logan, J., Abumrad, N.N., Hitzemann, R.J., Pappas, N.S., Pascani, K., 1997a. Dopamine D2 receptor availability in opiate-dependent subjects before and after naloxone-precipitated withdrawal. *Neuropsychopharmacology* 16, 174-182.
- Wang, H., Moriwaki, A., Wang, J.B., Uhl, G.R., Pickel, V.M., 1997b. Ultrastructural immunocytochemical localization of mu-opioid receptors in dendritic targets of dopaminergic terminals in the rat caudate-putamen nucleus. *Neuroscience* 81, 757-771.
- Watson, B.J., Taylor, L.G., Reid, A.G., Wilson, S.J., Stokes, P.R., Brooks, D.J., Myers, J.F., Turkheimer, F.E., Nutt, D.J., Lingford-Hughes, A.R., 2014. Investigating expectation and reward in human opioid addiction with [(11)C]raclopride PET. *Addict Biol* 19, 1032-1040.
- Yager, L.M., Garcia, A.F., Wunsch, A.M., Ferguson, S.M., 2015. The ins and outs of the striatum: role in drug addiction. *Neuroscience* 301, 529-541.
- Yamada, H., Aimi, Y., Nagatsu, I., Taki, K., Kudo, M., Arai, R., 2007. Immunohistochemical detection of L-DOPA-derived dopamine within serotonergic fibers in the striatum and the substantia nigra pars reticulata in Parkinsonian model rats. *Neurosci Res* 59, 1-7.
- Zhou, F.C., Lesch, K.P., Murphy, D.L., 2002. Serotonin uptake into dopamine neurons via dopamine transporters: a compensatory alternative. *Brain Res* 942, 109-119.

Figure Legends

Figure 1. Scatter plots for correlations between [^{18}F]fluorodopa uptake and [^{11}C]carfentanil binding in a priori defined anatomical ROIs: (A) the globus pallidus, (B) caudate nucleus and (C) putamen. [^{11}C]carfentanil BP_{ND} and [^{18}F]fluorodopa K_i values result from ROI-based analyses. Solid circles = PG patients, open circles = healthy controls.

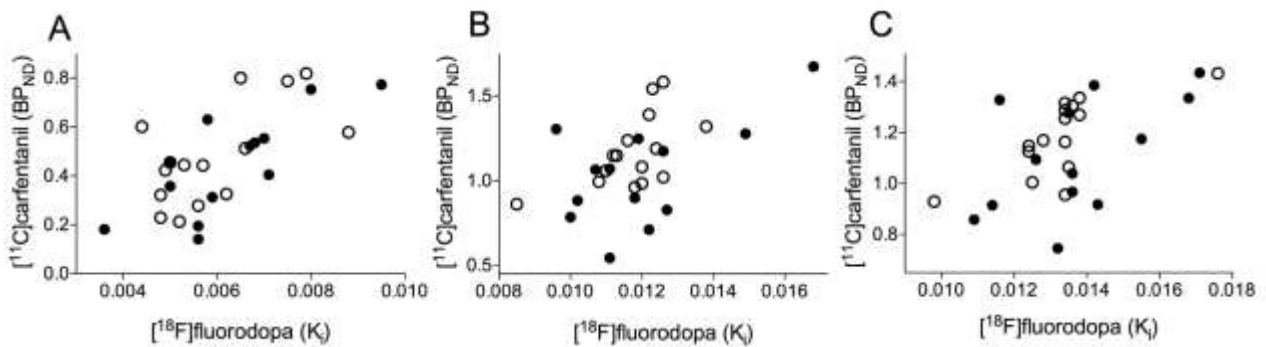
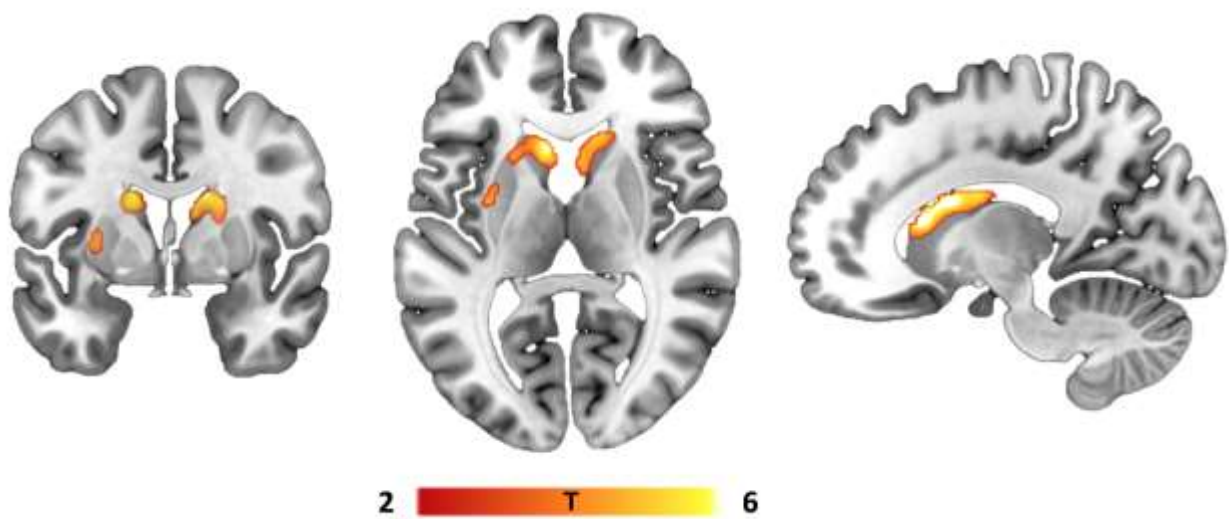


Figure 2. Significant clusters from the voxel-by-voxel analysis for the association between [^{18}F]fluorodopa and [^{11}C]carfentanil. Only significant clusters with family-wise error-corrected p values less than 0.05 with a cluster-forming threshold of $p < 0.001$ are shown.



Tables

Table 1. Demographic characteristics from the studied sample. Values are means (SD) or n (%). *P*-values are from independent samples *t*-tests or Fisher Exact tests.

	Healthy controls	Pathological gamblers	<i>p</i>
N	15	13	
Age	42.1 (11.1)	42.1 (12.2)	0.99
Sex (m/f)	7/8	7/6	1.0
Smoking (y/n)	6/9	10/3	0.067
BMI	24.7 (2.0)	25.0 (3.9)	0.81
AUDIT	5.6 (3.9)	6.1 (4.3)	0.75
BDI	2.7 (3.2)	4.5 (8.0)	<0.001
SOGS	0.07 (0.26)	13.5 (2.2)	<0.001
PG DSM-IV points	0.07 (0.26)	7.6 (1.3)	<0.001

BMI = body mass index, AUDIT = Alcohol Use Disorders Identification Test, BDI = Beck Depression Inventory, SOGS = South Oaks Gambling Screen, DSM-IV = DSM-IV diagnostic criteria for pathological gambling

Table 2. Intraregional correlations between [¹⁸F]fluorodopa *K_i* and [¹¹C]carfentanil BP_{ND}.

Region of interest	Healthy controls		Pathological gamblers		All subjects (N=28)		
	Spearman <i>r</i>	<i>p</i>	Spearman <i>r</i>	<i>p</i>	Spearman <i>r</i>	<i>p</i>	Bonferroni corrected <i>p</i>
Putamen	0.705	0.003	0.591	0.033	0.556	0.002	0.015
Caudate nucleus	0.580	0.024	0.267	0.38	0.461	0.014	0.095
Globus pallidus	0.550	0.034	0.715	0.006	0.610	0.001	0.004
Nucleus accumbens	0.355	0.19	0.011	0.97	0.107	0.59	
Amygdala	0.232	0.41	0.055	0.86	0.137	0.49	
Thalamus	0.114	0.69	0.544	0.055	0.323	0.094	
Hippocampus	-0.145	0.61	0.308	0.31	0.031	0.88	